



Classification of cancer images with CNN-based deep learning approach

CNN tabanlı derin öğrenme yaklaşımı ile kanser görüntülerinin sınıflandırılması

Halit Çetiner^{1,*} 

¹ Isparta University of Applied Sciences, Vocational School of Technical Sciences, 32000, Isparta Turkey

Abstract

Skin cancers known as melanoma (mel), dermatofibroma (df), and vascular (vasc), benign keratosis (bkl), melanocytic nevi (nv), basal cell carcinoma (bcc), actinic keratosis (akiec) have a high similarity. Accurate classification of specified skin cancers at an early stage is important in terms of saving human life. In this article, a high-accuracy deep learning model is proposed for the classification processes of common skin cancers. The proposed model is a model that helps skin specialists with a high workload and has rapid diagnosis and classification competence. A 30-layer CNN model is proposed that takes advantage of the swish and ReLU activation functions in the classification of highly similar skin cancers. Using this model, 0.99%, 0.99%, 0.96%, 0.99%, 0.92%, 0.99%, 0.95% F1 score values were obtained in the classification of skin cancers named akiec, bcc, bkl, df, nv, vasc, mel, respectively. In terms of precision and recall measurement metrics in the classification of skin cancers named Akiec, bcc, bkl, df, nv, vasc, mel, respectively, 0.99%, 0.99, 0.93, 0.99, 0.97, 0.99, 0.94 precision and 0.99, 0.98, 0.99, 1, 0.87, 1, 0.97 recall values were obtained. Based on the performance results obtained, it can be said that the proposed model correctly classifies seven very similar skin cancers.

Keywords: CNN, Random over sampler algorithm, Skin cancer, Deep learning

1 Introduction

In 2018, 9.6 million people died as a result of cancer cases [1]. It is reported that there is an increase in cancer cases due to various factors caused by lifestyle, genetic problems, air, water and soil pollution [2]. The number of people living on Earth is increasing day by day. The total number of people living on Earth is expected to reach ten billion in the coming years [3]. Parallel to this, various institutions and organizations, especially the World Health Organization (WHO), state that the diseases that impair human health have increased in the past ten years [4]. Pollution from water, air, and soil is among the factors that affect human health. As Pimentel et al. state, environmental degradation is considered the leading cause of death in the world today [4]. Major deaths occur as a result of air, water

Öz

Halk arasında melanoma (mel), dermatofibroma (df), ve vascular (vasc), bening keratosis (bkl), melanocytic nevi (nv), basal cell carcinoma (bcc), actinic keratosis (akiec) olarak bilinen cilt kanserleri yüksek benzerliğe sahiptir. Belirtilen cilt kanserlerinin erken aşamada doğru bir şekilde sınıflandırılması insan yaşamını kurtarması açısından önemlidir. Bu makalede yaygın görülen cilt kanserlerinin sınıflandırma süreçleri için yüksek doğruluklu bir derin öğrenme modeli önerilmiştir. Önerilen model, genel olarak iş yoğunluğu yüksek olan cilt uzmanlarına yardımcı, hızlı tanı ve sınıflandırma yetkinliğine sahip bir modeldir. Birbirine oldukça benzer olan cilt kanserlerinin sınıflandırılmasında, swish ve ReLU aktivasyon fonksiyonlarının avantajlarından faydalanan 30 katmanlı bir CNN modeli önerilmiştir. Bu model kullanılarak akiec, bcc, bkl, df, nv, vasc, mel adlı cilt kanserlerinin sınıflandırılmasında sırasıyla 0.99%, 0.99%, 0.96%, 0.99%, 0.92%, 0.99%, 0.95% F1 score değerleri elde edilmiştir. Akiec, bcc, bkl, df, nv, vasc, mel adlı cilt kanserlerinin sınıflandırılmasında precision ve recall ölçüm metrikleri açısından sırasıyla 0.99%, 0.99, 0.93, 0.99, 0.97, 0.99, 0.94 precision ve 0.99, 0.98, 0.99, 1, 0.87, 1, 0.97 recall değerleri elde edilmiştir. Elde edilen performans sonuçlarına göre önerilen modelin birbirine oldukça benzer yedi farklı cilt kanserini doğru bir şekilde sınıflandırdığı söylenebilir.

Anahtar kelimeler: CNN, Rastgele yeniden örnekleme algoritması, Cilt kanseri, Derin öğrenme

and soil pollution, malnutrition and the damage caused by humans to the environment. Beyond this, another factor that harms human health is considered tobacco-related smoke and indoor cooking [5]. There is an increase in the number of cancer cases related to the stated effect and environmental factors [4].

Although cancer cases are seen in various organs and tissues, there has recently been an increase in skin cancers [6]. The reason for the increase in skin cases is reported to be the effect of air, water and soil pollution [2], [7]. The depletion of the ozone layer, which occurs together with these pollutants, causes the harmful sun rays to directly harm people. As a result, an increase in the incidence of skin cancer is observed [8-10]. The skin is defined as the largest human superficial organ [11]. The skin serves to protect the

* Sorumlu yazar / Corresponding author, e-posta / e-mail: halitcetiner@isparta.edu.tr (H. Çetiner)

Geliş / Recieved: 14.07.2022 Kabul / Accepted: 09.11.2022 Yayınlanma / Published: 15.01.2023

doi: 10.28948/ngumuh.1143693

internal environment from the external environment in the event of possible attacks on human organs. In addition to these, skin helps to maintain the human body temperature under normal conditions. It provides the first precaution against diseases that will protect the body from a possible harmful sunlight. Allows the formation of vitamin D by providing the absorption of beneficial sun rays [11]. However, in case of exposure to excessive sunlight, damage to the skin surfaces may occur and abnormal proliferation may occur. In this case, the disease that starts on the skin surface can progress.

Analyzes should be carried out by detecting abnormalities on the skin surface in variable ways and structures. Medical analyzes can be performed on images of skin surfaces using different techniques. Within the scope of this article, skin cancer types such as akiec, bcc, bkl, df, mel, nv, and vasc are analyzed. It is important to treat other types, including the mel type, in the early stages before they become widespread. However, if the progression of skin lesions is detected late, the patient's survival chance decreases to 10% [12].

To solve the specified problem with artificial intelligence algorithms, research has been carried out. As a result of the research, it has been determined that traditional artificial neural network algorithms based on classical machine learning have difficulties in solving these problems [13]. For this reason, the analysis of different types of skin cancer images has been carried out with deep learning methods, which are very popular today. Deep learning allows to do original studies in many different disciplines such as natural language processing, emotion analysis, computer vision analysis, text analysis, voice recognition, biomedical image analysis [14–16]. Deep learning applications, which have not been widespread until today, have become widespread due to reasons such as the hardware being not very powerful. The reason for this expansion is not only the increase in hardware capabilities, but also the increase in data sets from different disciplines. A model based on Convolution Neural Networks (CNN) algorithms, which is a sub-field of deep learning, has been created to classify skin cancer types. In order to increase the success of the created model, the Random Over Sampler algorithm was run on the data set with data imbalance. As a result of its execution, data set imbalances were eliminated. Data number imbalances between classes are eliminated. The Random Over Sampler algorithm [17–19] is a successful algorithm that is actively used to resolve data set imbalances. Lu et al. [19] state that he used different data balancing algorithms to eliminate data imbalances in his research. However, they declare that the Random Over Sampler algorithm is more successful than the others. By increasing the class accuracy of this method, it has increased the recall, F1 score, precision values at the same rate.

In the literature, as well as architectural models based on pre-trained neural networks, skin cancer types can be classified with CNN models created by the succession of multiple layers of deep learning with a certain logic.

Brinker et al. report that it makes sense to use CNN-based models for the classification of skin lesions, as they perform well in small or large datasets of skin cancer [20]. However,

the fact that there are studies that are not open to use in the datasets used limit the comparison of the developed methods. For the stated reason, a CNN-based model has been developed that can be tested on a common data set. Approaches that provide a classification of CNN-based skin lesions in the literature were examined according to the specified theme. During the review, the data set used in this article and CNN studies on different data sets were evaluated.

Hosny et al. classified skin cancer types mel, nv, bcc, akiec, bkl, df, and vasc with an AlexNet-based CNN model [21]. The proposed model is trained on the ISIC 2018 dataset. In experimental studies, they achieved success rates of 98.70%, 95.60%, 99.27%, and 95.06%, respectively, in terms of parameters called accuracy, sensitivity, specificity, and precision. Melanoma-type skin cancer was classified with a deep CNN model proposed by Yu et al. [22]. They appear to use the residual learning approach that deals with extreme learning problems. It created a fully convolutional residual network-based model for classification. With the CNN-based model they created, they reached an average of 85.5% accuracy. For classification of skin lesions, Brinker et al. are based on CNN-based architectures VGG 16 and GoogleNet [20]. They developed two different CNN-based models with these underlying architectures. They achieved a classification rate of 79.7% with the VGG 16-based CNN model. The GoogleNet-based CNN model reached 81.5% classification rate.

Ramachandro et al. used the same data balancing algorithm and data set that we used in the article in their study [23]. However, in the study, it is seen that only images containing akiec, bcc, df and mel types are classified, not seven different types of skin cancer. With the CNN model they developed, it is seen that the accuracy, precision, recall, and F1 score performance metrics reached 93%, 91%, 89%, and 92% on average, respectively. Sae-Lim et al. used the same data set used in the article [24]. Performed data augmentation to balance the data in the data set. In the tests performed on the balanced data set with data augmentation, they achieved success results of 83.23%, 87%, 85% and 82%, respectively, in terms of accuracy, specificity, sensitivity, and F1 score with the MobileNet-based CNN model. In tests carried out without data augmentation, they achieved success rates of 83.93%, 81%, 84%, and 80%, respectively, in terms of accuracy, specificity, sensitivity, and F1 score performance criteria with the MobileNet-based model. Transferring from architectural models with high computational costs such as MobileNet, AlexNet, GoogleNet has an effect on the high results. One of the different aspects of the model proposed from these studies is that it was developed without using any transfer learning architecture. As the main effect of this, it can be said that the proposed model is lighter. At the same time, with the proposed model, very satisfactory results were obtained not only in accuracy but also in F1 score, recall and precision values. Another important difference of our study is that there is no big difference between accuracy, F1 score, recall, and precision values.

According to the principles stated in this study, the analysis was developed with a deep learning-based CNN model without using any pre-trained architectural structure. In pattern recognition and classification studies, CNN-based models facilitate the extraction of distinctive features. An effective feature extraction structure was created using seven different convolutional layers.

The main contributions of the article, which was carried out for this purpose, to the literature are given below.

- In the proposed CNN model, the ReLU activation-based hard swish (h-swish) activation function is used. In addition, it is aimed to improve the performance results. There is evidence that the h-swish activation function improves classification accuracy [25].
- The strengths of the swish and ReLU activation functions are used in the proposed CNN model consisting of 30 layers.
- With the proposed CNN model, a success score of 97.65% was achieved.

The following parts of the article consist of three different parts. In the first part, materials and methods used in experimental studies are presented in the article. In the second part, the performance metrics of the proposed CNN model are given. In the last section, concluding information about the article is presented.

2 Material and methods

2.1 Material

In article studies, the reliability and validity of the deep learning model depend on the data set. For this reason, a data set whose data were prepared by experts was preferred.

The data set preferred and used in the article was prepared in the Dermatology department of the country of Austria. There are 10015 images in the data set prepared by skin specialists from 2 different dermatology departments [26]. In this dataset, there are 7 classes with different targets named akiec, bcc, bkl, df, mel, nv, and vasc. Akiec, bcc, bkl, df, mel, nv, vasc target tags in this data set consist of 327, 514, 1089, 115, 1111, 6660, 142, respectively. Class distributions according to the specified target labels are shown in Figure 1. Nv, mel, bkl, bcc, akiec, vasc, df represent the number of images in labeled classes with numbers 4, 6, 2, 1, 0, 5, 3, respectively.

In Figure 1, the class distributions of the data set used in the experimental studies of the article are shown. The data set shown has uneven data distribution. When training is done in this way, there are imbalances and deficiencies. In order to increase the success of the created model, the Random Over Sampler algorithm was run on the data set with data imbalance. As a result of its operation, the imbalances in the data set were eliminated. Different results of experimental study performance are presented to examine whether it can be eliminated. The data set balanced with the Random Over Sampler algorithm is shown in Figure 2.

The Random Over Sampler algorithm applied to eliminate data number imbalances between classes is a successful algorithm that is used actively to eliminate data set imbalances [17–19]. Lu et al. [19], state that they used different data balancing algorithms, including the Random

Over Sampler algorithm, to eliminate data imbalances in their research. In addition, they declare that the Random Over Sampler algorithm is more successful than other data balancing algorithms. When increasing the class accuracy of this method, it is expected that it will increase the recall, the F1 score, and the precision values at the same rate. As a result of the experimental studies, significant results were obtained in parallel with expectations.

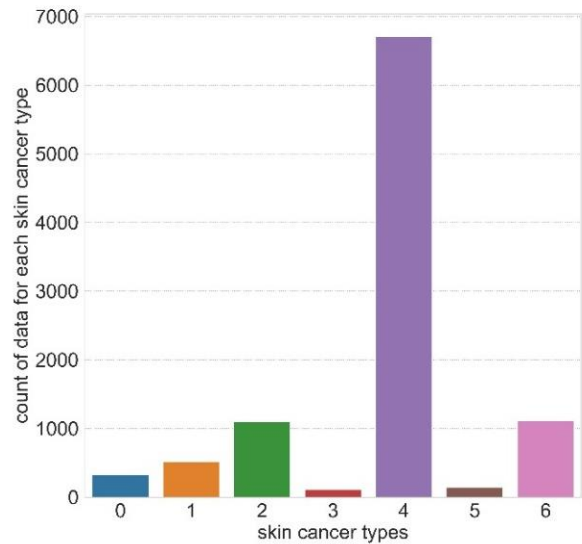


Figure 1. Data set in-class distributions

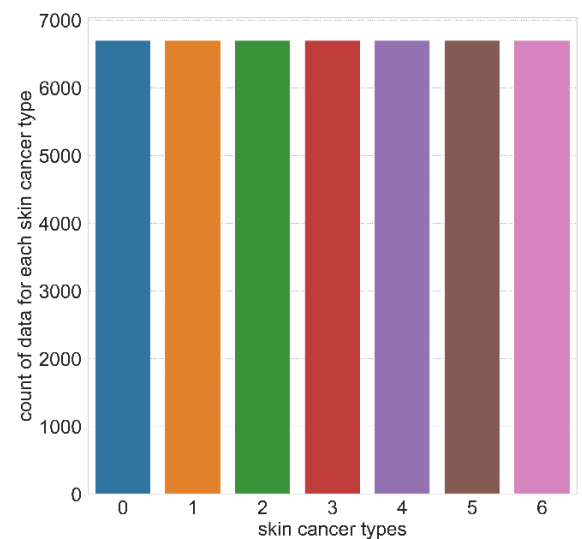


Figure 2. Balanced dataset distributions

2.2 The proposed CNN model

A CNN model is proposed for the automatic classification of skin cancer types. A CNN model consisting of 30 layers is proposed. The proposed model consists of four block structures. This block structure is simply shown in Figure 3. The detailed representation of the specified block structures is presented in Figure 4 and 5. As a result of combining the block 1 and block 2 structures presented in

Figure 4 and the block 3 and block 4 structures presented in Figure 5, 30 layers are formed.

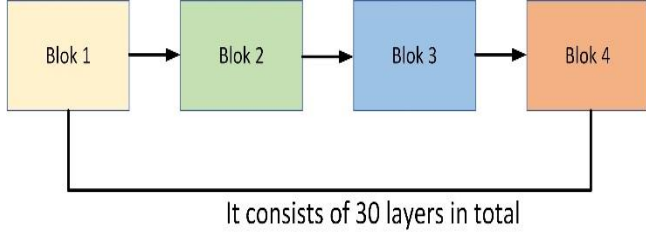


Figure 3. Block diagram of the proposed model

Since it would be complex to show all layers in a single Figure, the flow diagram of the proposed model is shown in blocks as indicated. In the first layer of the proposed model, 28x28x3 skin cancer images are given as input. Here 28x28 shows the width and height dimensions of the skin cancer images given as input. The images given as input have 3 color channels. Color channels are also presented to the model by multiplying with the input sizes. In 7 of the first 14 layers of the proposed model, the h-swish activation function is used instead of the ReLU activation function, which is used predominantly in different transfer learning-based architectures [27]. The ReLU activation function, one of its distinguishing features is that the input is a piecewise linear function in a multilayer deep learning network [28]. The Swish function is an activation function such as ReLU. The swish activation function with a sigmoid multiplier is shown in Equation (1).

$$swish(x) = x\sigma(x) \quad (1)$$

The ReLU activation function is widely used in the literature because it alleviates the gradient disappearance problem. ReLU activation function neurons fall into the hard saturation area during model training. As a result of this decrease, the weight values cannot be updated [29]. However, it is seen that it is used as a broadcast in quite different applications to be used in positive inputs [28–30]. At the same time, instead of activation functions such as tanh, arctan or sigmoid, it is used because the probability of gradient loss is reduced with the ReLU activation function [21]. The ReLU activation function is presented in Equation (2).

$$ReLU(x) = \max(0, x) \quad (2)$$

The sigmoid activation function is used in the function defined in Equation (1). Sigmoid activation has been transformed into a function called h-swish function due to its high computational cost. This function is given in Equation (3). According to Big O notation, the complexity of the work can be calculated in terms of time and algorithm [31]. Many input parameters such as the number of multiplications and additions in the convolution layers are considered to be constant so that the specified calculations can be made.

$$h - swish[x] = x \frac{ReLU6(x + 3)}{6} \quad (3)$$

In this case, a calculation was carried out to measure the effect of the ReLU and h-swish activation functions in the proposed model. In the specified function in Equation (3), the ReLU6 function is used instead of the sigmoid activation function with high processing load. Since the middle of 2019, it has been increasing its effectiveness with the h-swish non-linear activation function instead of ReLU. In the other layers, other than the first 7 layers, the ReLU activation function is used to benefit from the features of both activation functions that will increase the efficiency. In addition, in the proposed model, when the ReLU activation function is used instead of the h-swish activation function, an average performance degradation of 4% has been experienced. When its effectiveness was measured with the h-swish activation function, performance results close to Table 2 were obtained. However, the h-swish activation function is trained in more time than the ReLU activation function. The model with all ReLU activation function trained ten seconds faster than the model with all h-swish activation function. At this point, while the h-swish activation function is used in convolution layers, the ReLU activation function is used in other layers. In the distinction made, this method was used because it was desired to determine the experimental studies and the working separation of both activations. In addition, when activation functions are used with the mentioned approach, an increase of 1% in performance measures was observed compared to experimental studies with all h-swish activation. Using the block diagrams shown in Figure 4, the first part of the proposed model using swish activation was obtained by using the input layer, block 1, and 3 blocks 2. The convolution layers in block 1 were created using 32 filters with 2x2 window sizes. Two-dimensional maximum pooling is used in the maximum pooling layers with 2x2 window sizes. The stride value is defined as none in all Max pooling layers. In Block 2, convolution layers with 64, 128 and 256 2x2 window sizes were applied, respectively. At the same time, the stride values of the max pooling layer layers in block 2 are set to none. After the first parts of the proposed model were created from the specified blocks, it was transformed into a one-dimensional matrix with the Flatten layer.

In the second stage of the proposed model, upper layers with ReLU activation function were added. On top of the 14 layers of the structure specified in Figure 4, the blocks whose block diagrams are shown in Figure 5 were added. In blocks 3 and 4, the dropout layer was used, which performs 0.1 neuronal dropout. In the Dense layer, which was applied as the hidden neuron layer, 256 hidden neurons were used. Batch normalization was applied to normalize the input between the layers. In the last step, classification layer with softmax activation function is defined.

The structures defined in Figures 4 and 5 and the flow diagram of the proposed model are shown.

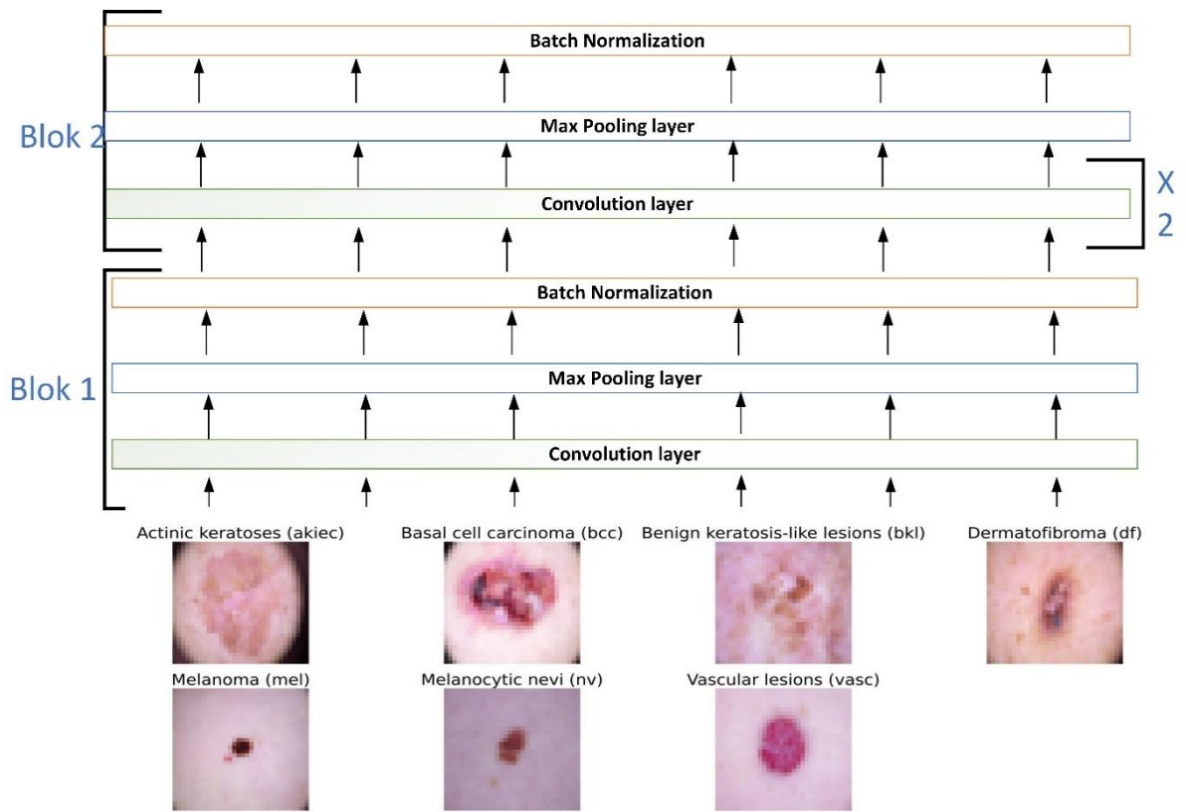


Figure 4. The proposed CNN model block 1 and block 2 diagrams

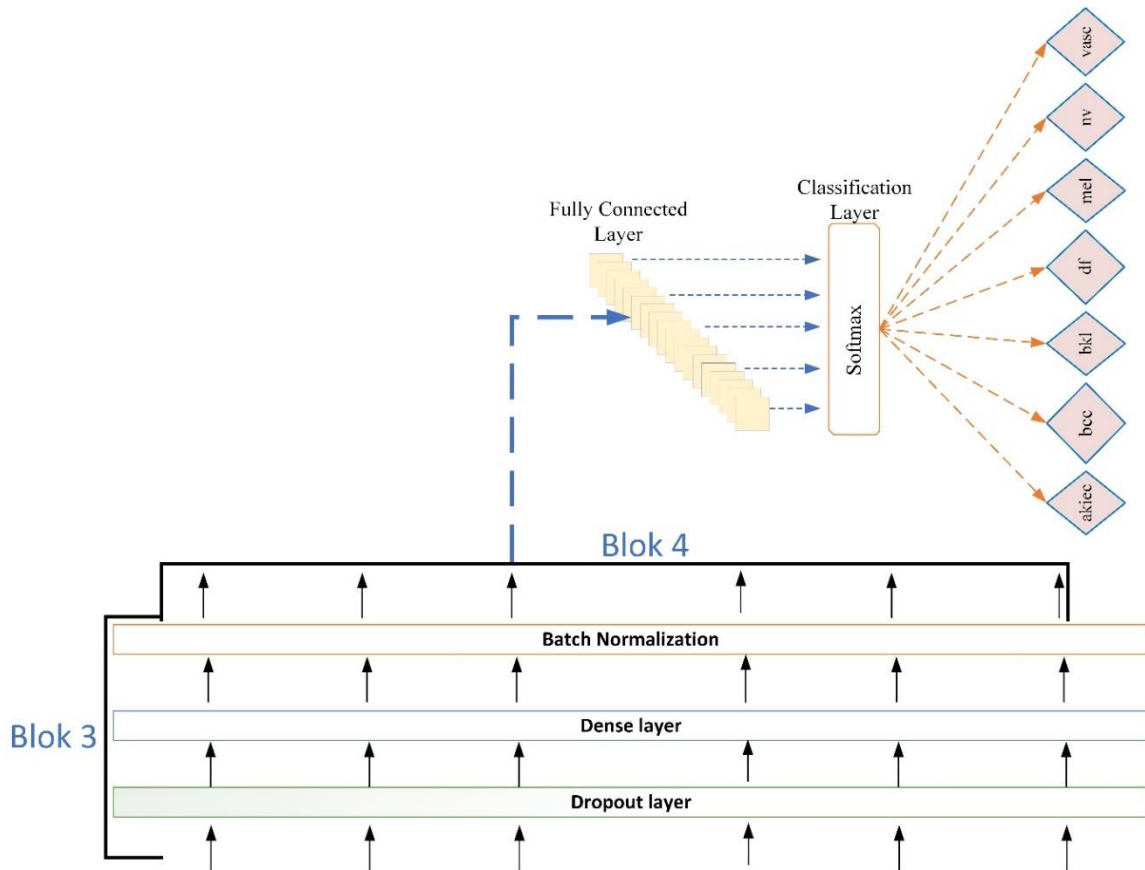


Figure 5. The proposed CNN block 3 and block 4 diagrams

Studies were carried out to determine the effectiveness of the proposed model according to the structures shown. The experimental studies carried out and the performance results obtained are evaluated in terms of F1 score, recall, precision, accuracy values, and presented in Section 3.

3 Results and discussion

The performance results of the proposed CNN model, which were obtained as a result of the experimental studies carried out on the data set with 7 different classes, are presented in this study. To obtain the best performance metrics, the first 14 layers of the proposed CNN model algorithm are shown with block 1 and block 2 block diagrams. The next layers are presented in detail with block 3 and block 4 block diagrams. That is, the first 14 layers are represented in blocks 1 and 2, while the remaining 16 layers are represented in blocks 3 and 4. The accuracy and loss graphs obtained from the experimental studies using the Adam optimization method with 15 iterations are presented in Figure 6 and Figure 7. Batch size value, which is one of the hyperparameters other than epoch, is also set to 128. The model is trained with Adam optimization method without any learning rate. The training and test accuracy graphs of the proposed CNN model are given in Figure 6. With the proposed CNN model, success rates of 98.67% and 97.65% were achieved, respectively, in terms of training and test accuracy.

There is a data imbalance between the types of skin cancer used in this article. Random Over Sampling method was used to eliminate this imbalance. Experimental studies have been carried out to measure whether dataset balancing is successful using this method. In Table 1, the results obtained without data balancing are given. As can be seen from the results, the imbalance between the types of data set greatly affects the performance results. For this reason, the data set is in a balanced state in the next steps of the study. The results obtained in all graphs and tables after Table 1 are the results obtained after data balancing.

Table 1. The performance results of the proposed CNN model without random over sampler

Skin types	Precision	Recall	F1 score
Akiec	0.60	0.27	0.37
Bcc	0.53	0.60	0.56
Bkl	0.59	0.33	0.42
Df	0.40	0.22	0.28
Nv	0.84	0.91	0.87
Vasc	0.91	0.37	0.53
Mel	0.46	0.41	0.44
Weighted average values	0.74	0.73	0.72

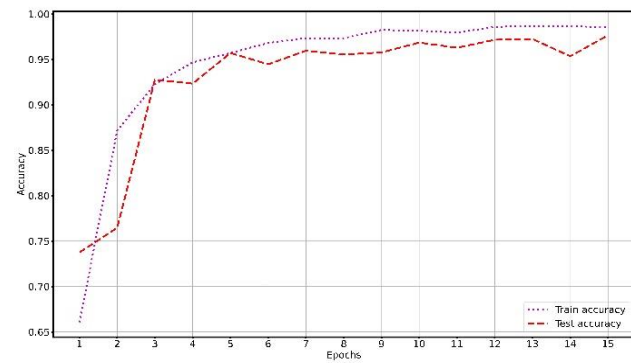


Figure 6. Graphs of training and testing accuracy of the proposed CNN model to classify skin cancer type

Table 2. The proposed CNN model performance results

Skin types	Precision	Recall	F1 score
Akiec	0.99	0.99	0.99
Bcc	0.99	0.98	0.99
Bkl	0.93	0.99	0.96
Df	0.99	1	0.99
Nv	0.97	0.87	0.92
Vasc	0.99	1	0.99
Mel	0.94	0.97	0.95
Weighted average values	0.97	0.97	0.97

The training and test losses obtained by using the proposed CNN model were 0.03%, 0.09%, respectively.

The results of the proposed CNN model with 15 iterations are given in Table 2. According to the given table, the F1 score points in akiec, bcc, df, and vasc classes are quite high. The recall values of the df and vasc classes were higher than the other classes. The precision values of the Akiec, bcc, df, and vasc classes were higher than those of the other classes. When examined in general, the results obtained are close to each other, but at a satisfactory level.

Average precision, recall, and F1 score values reached 97%. With these results, confusion matrix results are presented in order to show in detail that the performance of the proposed CNN model is good. The results of the confusion matrix presented are given in Figure 8. How many misdiagnoses in which classes are all presented in Figure 8.

The skin cancer images shown in Figure 9 are given as input to the proposed CNN model. Estimated and actual target class label numbers obtained as a result of giving are shown. The target tag numbers here are class tags with numbers 4, 6, 2, 1, 0, 5, 3 respectively, nv, mel, bkl, bcc, akiec, vasc, df.

According to the performance results of the proposed CNN model, feature-based skin cancer classification study [32], color and tissue lesion-based descriptive method [33], CNN model with logistic regression classifier [34] got high

results. According to the results obtained, the test accuracy rate of the proposed CNN model has an accuracy difference of 16.65%, 16.65%, 18.85% from the studies [32], [33] and [34], respectively. With these results, the proposed CNN model has proven success with training, test accuracy, and loss graphs. At the same time, together with the confusion matrix, it allowed the results obtained on a class basis to be examined in detail. In Table 3, a comparison of the proposed model with similar data sets is presented. The proposed model performed as strong as the studies in the literature.

Table 3. Comparison of the proposed model with studies using similar data sets

Author	Precision	Recall	F1 score	Accuracy
Ramachandro et al. [23]	91%	89%	92%	93%
Sae-Lim et al. [24] with data augmentation	-	85%	82%	83.23%
Sae-Lim et al. [24] without data augmentation	-	84%	80%	83.93%
Proposed model	97%	97%	97%	97.65%

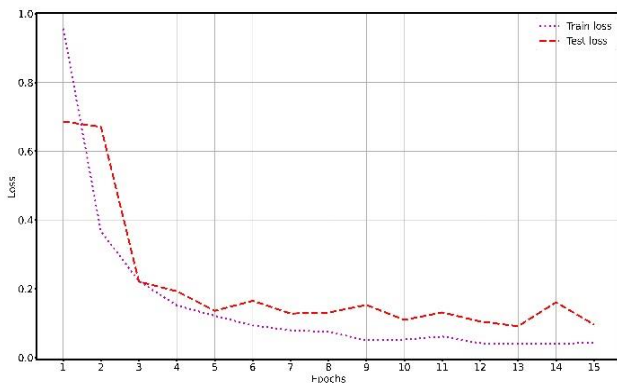


Figure 7. Training and test loss plots of the proposed CNN model

4 Conclusions

Ozone layer depletion, which occurs due to the increase in environmental pollution, is a subject of research by scientists. Because as a result of ozone layer damage, the amount of exposure to harmful sun rays that radiate at different wavelengths increases. For such reasons, in this article a system is proposed that automatically classifies skin cancers that can be seen in different age ranges. In general, there are 30 deep learning layers in the proposed structure. The proposed CNN model is developed using a lightweight, computationally inexpensive swish activation function. The Random Over Sampler algorithm, which contributed to the elimination of the imbalance of the data set, also had an effect on the performance results obtained. When the obtained F1 score, recall, precision, and accuracy values are examined, it is seen that the results are close to each other.

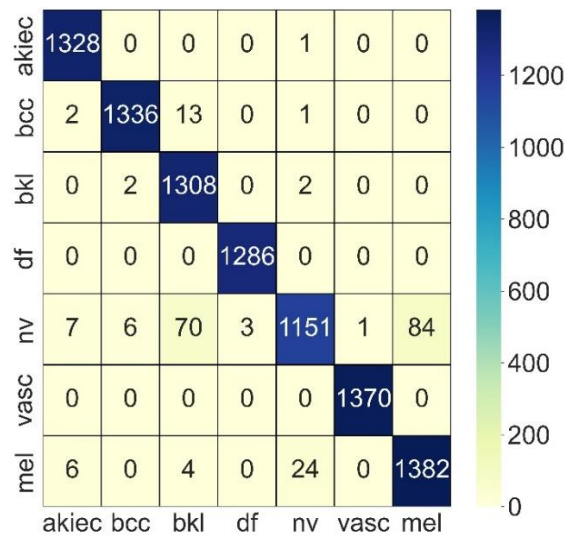


Figure 8. The proposed CNN model confusion matrix

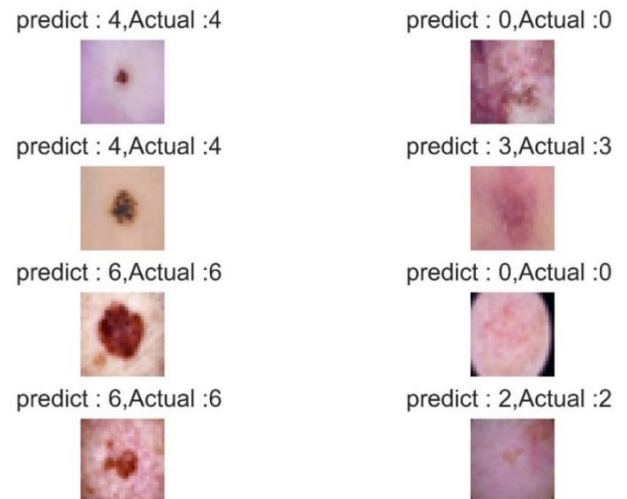


Figure 9. Test results obtained with the proposed CNN model

Conflict of interest

The authors declare that there is no conflict of interest.

Similarity rate: 6%

References

- [1] H. Younis, M. H. Bhatti, and M. Azeem, Classification of Skin Cancer Dermoscopy Images using Transfer Learning, in 2019 15th International Conference on Emerging Technologies, 1–4. 2019. <https://doi.org/10.1109/ICET48972.2019.8994508>.
- [2] C. De Martel, J. Ferlay, S. Franceschi, J. Vignat, F. Bray, D. Forman, and M. Plummer, Global burden of cancers attributable to infections in 2008: a review and synthetic analysis, *Lancet Oncol.*, 13(6), 607–615, 2012.
- [3] R. Perroy, World population prospects, United Nations, 1(6042), 587–592, 2015.

- [4] D. Pimentel, S. Cooperstein, H. Randell, D. Filiberto, S. Sorrentino, B. Kaye, C. Nicklin, J. Yagi, J. Brian, J. O'Hern, A. Habas, and Weinstein, Ecology of Increasing Diseases: Population Growth and Environmental Degradation, *Hum. Ecol. Interdiscip. J.*, 35(6), 653–668, 2007. <https://doi.org/10.1007/s10745-007-9128-3>.
- [5] N. Bruce, R. Perez-Padilla, and R. Albalak, The health effects of indoor air pollution exposure in developing countries, *Geneva World Heal. Organ.*, 11, 2002.
- [6] U.-O. Dorj, K.-K. Lee, J.-Y. Choi, and M. Lee, The skin cancer classification using deep convolutional neural network, *Multimed. Tools Appl.*, 77(8), 9909–9924, 2018. <https://doi.org/10.1007/s11042-018-5714-1>.
- [7] K. E. Kim, D. Cho, and H. J. Park, Air pollution and skin diseases: Adverse effects of airborne particulate matter on various skin diseases, *Life Sci.*, 152, 126–134, 2016.
- [8] A. J. McMichael and T. McMichael, *Planetary overload: global environmental change and the health of the human species*. Cambridge University Press, 1993.
- [9] P. Martens and A. J. McMichael, *Environmental change, climate and health: issues and research methods*. Cambridge University Press, 2009.
- [10] R. L. McKenzie, L. O. Björn, A. Bais, and M. Ilyas, Changes in biologically active ultraviolet radiation reaching the Earth's surface, *Photochem. Photobiol. Sci.*, 2(1), 5–15, 2003.
- [11] F. W. Alsaade, T. H. H. Aldhyani, and M. H. Al-Adhaileh, Developing a Recognition System for Diagnosing Melanoma Skin Lesions Using Artificial Intelligence Algorithms., *Comput. Math. Methods Med.*, 9998379, 2021. <https://doi.org/10.1155/2021/9998379>.
- [12] D. B. Mendes and N. C. da Silva, Skin lesions classification using convolutional neural networks in clinical images, *arXiv Prepr. arXiv1812.02316*, 2018.
- [13] Y. LeCun, Y. Bengio, and G. Hinton, Deep learning, *Nature*, 521(7553), 436–444, 2015. <https://doi.org/10.1038/nature14539>.
- [14] M. Choudhary, S. S. Chouhan, E. S. Pilli, and S. K. Vipparthi, BerConvoNet: A deep learning framework for fake news classification, *Appl. Soft Comput.*, 110, 107614, 2021. <https://doi.org/10.1016/j.asoc.2021.107614>.
- [15] T. Chen, R. Xu, Y. He, and X. Wang, Improving sentiment analysis via sentence type classification using BiLSTM-CRF and CNN, *Expert Syst. Appl.*, 72, 221–230, 2017. <https://doi.org/10.1016/j.eswa.2016.10.065>.
- [16] X. Xu, L. Zhang, J. Li, Y. Guan, and L. Zhang, A Hybrid Global-Local Representation CNN Model for Automatic Cataract Grading, *IEEE J. Biomed. Heal. Informatics*, 24(2), 556–567, 2020, <https://doi.org/10.1109/JBHI.2019.2914690>.
- [17] A. Nabil, M. Seyam, and A. Abou-Elfetouh, Deep Neural Networks for Predicting Students' Performance, in *Proceedings of the 52nd ACM Technical Symposium on Computer Science Education*, 2021. <https://doi.org/10.1145/3408877.3439685>.
- [18] J. Liu, K. Li, B. Song, and L. Zhao, A Multi-stream Convolutional Neural Network for Micro-expression Recognition Using Optical Flow and {EVM}, *CoRR*, 2020.
- [19] W. Lu, H. Hou, and J. Chu, Feature fusion for imbalanced ECG data analysis, *Biomed. Signal Process. Control*, 41, 152–160, 2018. <https://doi.org/10.1016/j.bspc.2017.11.010>.
- [20] B. Titus Josef, H. Achim, U. Jochen Sven, G. Niels, S. Dirk, K. Joachim, B. Carola, S. Theresa, E. Alexander, and V. Christof, Skin cancer classification using convolutional neural networks: systematic review, *J. Med. Internet Res.*, 20(10), 2018.
- [21] K. M. Hosny, M. A. Kassem, and M. M. Fouad, "Classification of Skin Lesions into Seven Classes Using Transfer Learning with AlexNet, *J. Digit. Imaging*, 33(5), 1325–1334, 2020. <https://doi.org/10.1007/s10278-020-00371-9>.
- [22] L. Yu, H. Chen, Q. Dou, J. Qin, and P.-A. Heng, Automated Melanoma Recognition in Dermoscopy Images via Very Deep Residual Networks, *IEEE Trans. Med. Imaging*, 36(4), 994–1004, 2017. <https://doi.org/10.1109/TMI.2016.2642839>.
- [23] M. Ramachandro, T. Daniya, and B. Saritha, Skin Cancer Detection Using Machine Learning Algorithms, in *2021 Innovations in Power and Advanced Computing Technologies*, , 1–7, 2021. <https://doi.org/10.1109/i-PACT52855.2021.9696874>.
- [24] W. Sae-Lim, W. Wettayaprasit, and P. Aiyarak, Convolutional Neural Networks Using MobileNet for Skin Lesion Classification, in *2019 16th International Joint Conference on Computer Science and Software Engineering*,. 242–247, 2019. <https://doi.org/10.1109/JCSSE.2019.8864155>.
- [25] A. M. Alhassan and W. M. N. W. Zainon, Brain tumor classification in magnetic resonance image using hard swish-based RELU activation function-convolutional neural network, *Neural Comput. Appl.*, 33(15), 9075–9087, 2021. <https://doi.org/10.1007/s00521-020-05671-3>.
- [26] P. Tschandl, C. Rosendahl, and H. Kittler, The HAM10000 dataset, a large collection of multi-source dermatoscopic images of common pigmented skin lesions, *Sci. data*, 5(1), 1–9, 2018.
- [27] S. Qian, C. Ning, and Y. Hu, MobileNetV3 for Image Classification, in *2021 IEEE 2nd International Conference on Big Data, Artificial Intelligence and Internet of Things Engineering*, 490–497, 2021. <https://doi.org/10.1109/ICBAIE52039.2021.9389905>.
- [28] K. Eckle and J. Schmidt-Hieber, A comparison of deep networks with ReLU activation function and linear spline-type methods, *Neural Networks*, 110, 232–242, 2019. <https://doi.org/10.1016/j.neunet.2018.11.005>.
- [29] G. Lin and W. Shen, Research on convolutional neural network based on improved Relu piecewise activation function, *Procedia Comput. Sci.*, 131, 977–984, 2018. <https://doi.org/10.1016/j.procs.2018.04.239>.

- [30] Y. Yu, K. Adu, N. Tashi, P. Anokye, X. Wang, and M. A. Ayidzoe, RMAF: Relu-Memristor-Like Activation Function for Deep Learning, *IEEE Access*, 8, 72727–72741, 2020. <https://doi.org/10.1109/ACCESS.2020.2987829>.
- [31] S. Rubinstein-Salzedo, Big o notation and algorithm efficiency, in *Cryptography*, Springer, 75–83, 2018.
- [32] S.-R.-S. Jianu, L. Ichim, D. Popescu, and O. Chenaru, Advanced Processing Techniques for Detection and Classification of Skin Lesions, in 2018 22nd International Conference on System Theory, Control and Computing, 498–503, 2018. <https://doi.org/10.1109/ICSTCC.2018.8540732>.
- [33] I. Giotis, N. Molders, S. Land, M. Biehl, M. F. Jonkman, and N. Petkov, MED-NODE: A computer-assisted melanoma diagnosis system using non-dermoscopic images, *Expert Syst. Appl.*, 42(19), 6578–6585, 2015.
- [34] J. Kawahara, A. BenTaieb, and G. Hamarneh, Deep features to classify skin lesions, in 2016 IEEE 13th international symposium on biomedical imaging, 1397–1400, 2016. <https://doi.org/10.1109/ISBI.2016.7493528>.

